

---

# Conditional Diffusion Probabilistic Models for Super Resolution Microscopy

---

Anonymous Author(s)

Affiliation

Address

email

## Abstract

1 Single-molecule localization microscopy (SMLM) techniques are a mainstay of  
2 fluorescence microscopy and can be used to produce a pointillist representation  
3 of living cells at diffraction-unlimited precision. Classical SMLM approaches  
4 leverage the deactivation of fluorescent tags, followed by spontaneous or pho-  
5 toinduced reactivation, which can be used to estimate of the density of a tagged  
6 biomolecule in cellular compartments. Standard SMLM localization algorithms  
7 based on maximum likelihood estimators or least squares optimization require  
8 tight control of activation and reactivation to maintain sparse emitters, present-  
9 ing a tradeoff between imaging speed and labeling density. Deep models have  
10 generalized SMLM to densely labeled structures, yet uncertainty quantification  
11 is still lacking. Recently, denoising diffusion probabilistic models (DDPMs) have  
12 been adapted conditional super resolution tasks, demonstrating promising results  
13 in detail reconstruction, while directly providing uncertainties in model predictions.  
14 Here, we adapt DDPM to the task of single molecule localization, and demonstrate  
15 that DDPM approaches the Cramer-Rao lower bound on localization uncertainty  
16 over a wide range of experimental conditions.

## 17 1 Introduction

18 Single molecule localization microscopy (SMLM) relies on the temporal resolution of fluorophores  
19 whose spatially overlapping point spread functions would otherwise render them unresolvable at the  
20 detector. Common strategies for the temporal separation of molecules involve transient intramolecular  
21 rearrangements to switch from dark to fluorescent states or the exploitation of non-emitting molecular  
22 radicals. Estimation of molecular coordinates in SMLM is achieved by modeling the optical impulse  
23 response of the imaging system. However, dense localization suffers from the curse of dimensionality  
24 - the parameter space volume grows exponentially with the number of molecules, which is often  
25 unknown a priori. Exploration of this high dimensional parameter space in dense SMLM is often  
26 intractable.

27 Previous approaches to this issue has been to predict super-resolution images from a sparse set of  
28 localizations with conditional generative adversarial networks (Ouyang 2018) or direct prediction of  
29 coordinates using deep neural networks (Nehme 2020; Speiser 2021). However, diffusion models are  
30 an appealing alternative because they infer a distribution of deconvolved images that are compatible  
31 with an observation. Although conditional VAEs and conditional GANs can provide a distribution of  
32 deconvolved images, both are known to suffer from mode collapse and produce insufficient diversity  
33 in their outputs. Diffusion models are a recently developed alternative to VAEs and GANs that excel  
34 at producing diverse samples and have been successfully applied to solve inverse problems. Here, we  
35 present a novel diffusion model for deconvolution in single molecule localization microscopy.

36 Denoising diffusion probabilistic models (DDPM) have emerged as powerful generative models,  
 37 exceeding GANs and VAEs in a variety of generative modeling tasks. Nevertheless, learning diffusion  
 38 models directly in data space can limit expressivity of the model (Vahdat 2021). Therefore, we build  
 39 on previous approaches by using a CNN to compute a latent representation  $\mathbf{z}_i$ . A denoising diffusion  
 40 probabilistic model (DDPM) is then used to model the distribution  $P_\Phi(\mathbf{y}|\mathbf{z})$ .

41 Inversion of the degradation function  $F$  is generally intractable, particularly when fluorescent  
 42 molecules are dense within the field of view. This difficulty arises because the parameter  $\theta$  is  
 43 typically of large and unknown dimension, rendering maximum likelihood estimation or Markov  
 44 Chain Monte Carlo sampling computationally difficult. Previous solutions to this problem leverage  
 45 convolutional neural networks (CNNs) to infer coordinates directly by learning a deterministic im-  
 46 age transformation  $F^{-1}$ , which we refer to as a "localization map" (Nehme 2021). Such methods  
 47 faithfully capture the information content in degraded images; however, such methods apply arbitrary  
 48 thresholding to the CNN localization map, potentially creating erroneous localizations, and do not  
 49 permit sampling.

50 We seek a generative approach, which casts localization as an image restoration problem, where a  
 51 high resolution kernel density estimate  $\mathbf{y}$  is reconstructed from a low resolution image  $\mathbf{x}$ . Building  
 52 on previous efforts, we utilize a CNN learns a representation which compresses  $\mathbf{x}$  while preserving  
 53 the relevant information to the prediction of  $\mathbf{y}$ .

## 54 2 Denoising Diffusion Probabilistic Model for SMLM

55 We consider datasets  $(\theta_i, \mathbf{x}_i, \mathbf{y}_i)_{i=1}^N$  of observed images  $\mathbf{x}_i$  and kernel density estimate (KDE)  
 56 images  $\mathbf{y}_i$ , given an underlying set of object coordinates  $\theta_i$ . Observations  $\mathbf{x}_i$  are generated from  
 57  $\theta_i = (r_1, \dots, r_N)$  under an image degradation model  $F$ . We aim to develop a framework for  
 58 sampling from  $p(\mathbf{y}_i|\mathbf{x}_i)$  and inference of  $\theta_i$ , while fulfilling a resolution criterion under the condition  
 59  $|r_i - r_j| \geq \epsilon; \forall(i, j)$ .

### 60 2.1 Degradation Model

61 The central objective of single molecule localization microscopy is to infer a set of molecular  
 62 coordinates  $\theta$  from noisy, low resolution images  $\mathbf{x}$ . We therefore begin by defining the likelihood on  
 63 measured low-resolution images  $p(\mathbf{x}|\theta)$ . In fluorescence microscopy, each pixel is a Poisson random  
 64 variable (Smith 2010; Nehme 2020; Chao 2016), with expected value

$$\omega = i_0 \int O(u) du \int O(v) dv \quad (1)$$

65 where  $i_0 = \eta N_0 \Delta$ . The scalar parameters  $\eta, \Delta$  are the photon detection probability of the sensor and  
 66 the exposure time, respectively. Without loss of generality, we assume  $\eta = \Delta = 1$ . Most importantly,  
 67  $N_0$  represents the signal amplitude, which we assume maintains a fixed value. The optical impulse  
 68 response  $O(u, v)$  is often approximated as a 2D isotropic Gaussian with standard deviation  $\sigma$  (Zhang  
 69 2007). This approximation has the convenient property, that the effects of pixelation can be expressed  
 70 in terms of error functions. For example, given a fluorescent emitter located at  $\theta = (u_0, v_0)$ , we have  
 71 that

$$\int O(u) du = \frac{1}{2} \left( \operatorname{erf} \left( \frac{u_k + \frac{1}{2} - u_0}{\sqrt{2}\sigma} \right) - \operatorname{erf} \left( \frac{u_k - \frac{1}{2} - u_0}{\sqrt{2}\sigma} \right) \right) \quad (2)$$

72 where we have used the common definition  $\operatorname{erf}(z) = \frac{2}{\sqrt{\pi}} \int_0^t e^{-t^2} dt$ . Our generative model also  
 73 incorporates a normally distributed white noise per pixel  $\zeta$  with offset  $o$  and variance  $\sigma^2$ . Ultimately,  
 74 we have a Poisson component of the signal, which scales with  $N_0$  and a Gaussian component, which  
 75 does not. Therefore, in a single exposure, we measure:

$$\mathbf{x} = \mathbf{s} + \zeta \quad (3)$$

76 The distribution of  $\mathbf{x}$  is the convolution of the distributions of  $\mathbf{s}$  and  $\zeta$ ,

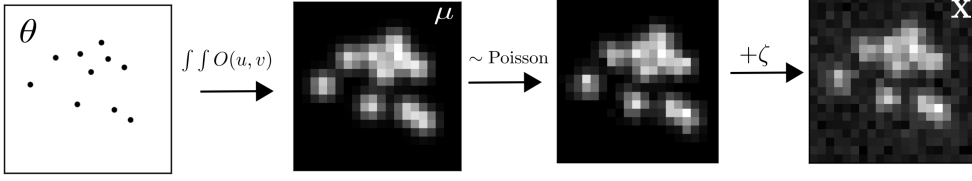


Figure 1: Generative model of single molecule localization microscopy images

$$p(\mathbf{x}_k|\theta) = A \sum_{q=0}^{\infty} \frac{1}{q!} e^{-\omega_k} \omega_k^q \frac{1}{\sqrt{2\pi}\sigma_k} e^{-\frac{(\mathbf{x}_k - g_k q - o_k)^2}{2\sigma_k^2}} \quad (4)$$

where  $p(\zeta_k) = \mathcal{N}(o_k, \sigma_k^2)$  and  $p(s_k) = \text{Poisson}(\omega_k)$ ,  $A$  is some normalization constant. In practice, (4) is difficult to work with, so we look for an approximation. We will use a Poisson-Normal approximation for simplification. Consider,

$$\zeta_k - o_k + \sigma_k^2 \sim \mathcal{N}(\sigma_k^2, \sigma_k^2) \approx \text{Poisson}(\sigma_k^2) \quad (5)$$

Since  $\mathbf{x}_k = \mathbf{s}_k + \zeta_k$ , we transform  $\mathbf{x}'_k = \mathbf{x}_k - o_k + \sigma_k^2$ , which is distributed according to

$$\mathbf{x}'_k \sim \text{Poisson}(\omega'_k) \quad (6)$$

where  $\omega'_k = \omega_k + \sigma_k^2$ . This result can be seen from the fact the convolution of two Poisson distributions is also Poisson. We then arrive at the following log likelihood

$$\ell(\mathbf{x}|\theta) = -\log \prod_k \frac{e^{-(\mu'_k)} (\mu'_k)^{n_k}}{n_k!} \approx \sum_k n_k \log n_k + \mu'_k - n_k \log (\mu'_k) \quad (7)$$

## 2.2 Fisher Information Metric

We use the Fisher information as an information theoretic criteria to assess the quality of the proposed algorithms, with respect to the root mean squared error (RMSE) of our predictions of  $\theta$ . The generative model  $\ell(\mathbf{x}|\theta)$  is also convenient for computing the Fisher information matrix (Smith 2010) and thus the Cramer-Rao lower bound, which bounds the variance of a statistical estimator of  $\theta$ , from below i.e.,  $\text{var}(\hat{\theta}) \geq I^{-1}(\theta)$ . It is shown in the appendix, that the Fisher information is straightforward to compute under the Poisson likelihood (7)

$$\mathcal{I}_{ij}(\theta) = \mathbb{E}_{\theta} \left( \frac{\partial \ell}{\partial \theta_i} \frac{\partial \ell}{\partial \theta_j} \right) = \sum_k \frac{1}{\omega'_k} \frac{\partial \omega'_k}{\partial \theta_i} \frac{\partial \omega'_k}{\partial \theta_j} \quad (8)$$

## 3 Conditional Denoising Diffusion Model

Given datasets  $(\theta_i, \mathbf{x}_i, \mathbf{y}_i)_{i=1}^N$  which represent samples drawn from an unknown conditional distribution  $p(\mathbf{y}|\mathbf{x})$ . This is a one-to-many mapping in which many target images may be consistent with an input image. The conditional DDPM model generates a target image  $y_0$  in  $T$  refinement steps. Starting with a pure noise image  $y_T \sim \mathcal{N}(0, I)$ , the model iteratively refines the image through successive iterations according to learned conditional transition distributions  $p(y_{t-1}|y_t, x)$  such that  $y_0 \sim p(\mathbf{y}|\mathbf{x})$

### 3.1 Gaussian Diffusion

Diffusion models (Sohl-Dickstein 2015; Ho 2020) are a class of generative models inspired by nonequilibrium statistical physics, which slowly destroy structure in a data distribution  $p(\mathbf{y}_0|\mathbf{x})$  via

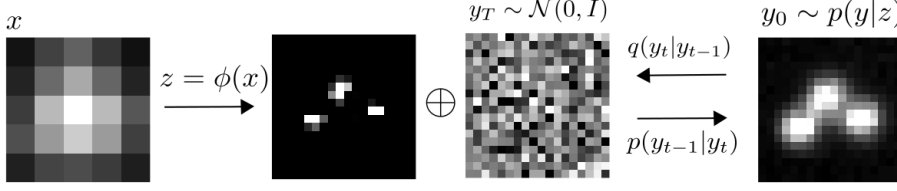


Figure 2: Conditional diffusion model for sampling kernel density estimates

100 a fixed Markov chain referred to as the *forward process*. In essence, the forward process gradually  
 101 adds Gaussian noise to the data according to a variance schedule  $\beta_{0:T}$

$$q(\mathbf{y}_t|\mathbf{y}_0) = \prod_{t=1}^T q(\mathbf{y}_t|\mathbf{y}_{t-1}) \quad q(\mathbf{y}_t|\mathbf{y}_{t-1}) = \mathcal{N}\left(\sqrt{1-\beta_t}\mathbf{y}_{t-1}, \beta_t I\right) \quad (9)$$

102 An important property of the forward process is that it admits sampling  $x_t$  at an arbitrary timestep  $t$   
 103 in closed form (Ho 2020). Using the notation  $\alpha_t := 1 - \beta_t$  and  $\gamma_t := \prod_{s=1}^t \alpha_s$ , we have

$$q(\mathbf{y}_t|\mathbf{y}_0) = \mathcal{N}(\sqrt{\gamma_t}\mathbf{y}_0, (1-\gamma_t)I) \quad (10)$$

104 The usual procedure is then to learn a parametric representation of the *reverse process*, and therefore  
 105 generate samples from  $p(\mathbf{y}_0)$ , starting from noise. Here, we are concerned with conditional diffusion  
 106 models, which instead sample from a conditional distribution  $p(\mathbf{y}_0|\mathbf{x})$ . Formally,  $p_\theta(\mathbf{y}_0|\mathbf{x}_0) =$   
 107  $\int p_\theta(\mathbf{y}_{0:T}|\mathbf{x}_0)d\mathbf{x}_{1:T}$  where  $y_t$  is a latent representation with the same dimensionality of the data.  
 108  $p_\theta(\mathbf{y}_{0:T}|\mathbf{x})$  is a Markov process, starting from a noise sample  $p_\theta(y_T) = \mathcal{N}(0, I)$ .

$$p_\theta(\mathbf{y}_{0:T}) = p_\theta(\mathbf{y}_T) \prod_{t=1}^T p_\theta(\mathbf{y}_{t-1}|\mathbf{y}_t) \quad p_\theta(\mathbf{y}_{t-1}|\mathbf{y}_t) = \mathcal{N}(\mu_\theta(\mathbf{y}_t), \beta_t I) \quad (11)$$

109 where we reuse the variance schedule of the forward process (Ho 2020). We seek to learn a denoising  
 110 model  $\mu_\theta$  which computes the mean of the Gaussian transition density at each time step  $t$ . However,  
 111 learning diffusion models directly in data space can limit expressivity of the model (Vahdat 2021).  
 112 Since we are primarily interested in learning a restoration  $\mathbf{y}$ , we choose to define an encoder  $\phi$  such  
 113 that  $\mathbf{z} = \phi(\mathbf{x}_0)$ . The reverse process then becomes  $p_\theta(\mathbf{y}_0|\mathbf{z} = \phi(\mathbf{x}_0)) = \int p_\theta(\mathbf{y}_{0:T}|\mathbf{z})d\mathbf{x}_{1:T}$ . For all  
 114  $t > 0$ , the mean of the transition density is computed as

$$\mu_\theta(\mathbf{y}_t, \mathbf{x}, \gamma_t) = \frac{1}{\sqrt{\alpha_t}} \left( \mathbf{y}_t - \frac{(1-\alpha_t)}{\sqrt{1-\gamma_t}} f_\theta(\mathbf{y}, \mathbf{x}, \gamma_t) \right) \quad (12)$$

115 where  $f_\theta$  is a neural network. Only at  $t = 0$  is this mean directly a function of  $\mathbf{x}$ .

### 116 3.2 Optimization of the Denoising Model

117 To reverse the diffusion process, we utilize an encoding  $\mathbf{z} = \phi(\mathbf{x})$  and optimize a neural denoising  
 118 model  $f_\theta$  that takes as input  $\mathbf{z}$  and a noisy target image  $\mathbf{y}_t \sim q(\mathbf{y}_t|\mathbf{y}_0)$ ,

$$\mathbf{y}_t = \sqrt{\gamma_t}\mathbf{y}_0 + \sqrt{1-\gamma_t}\epsilon, \quad \epsilon \sim \mathcal{N}(0, I) \quad (13)$$

119 This definition of a noisy target image  $\mathbf{y}_t$  is drawn from the marginal distribution of noisy images at  
 120 a time step  $t$  of the forward diffusion process. In addition to a source image  $\mathbf{y}_0$  and a noisy target  
 121 image  $\mathbf{y}_t$ , the denoising model  $f_\theta$  takes as input the sufficient statistics for the variance of the noise  
 122  $\gamma$ , and is trained to predict the noise vector  $\epsilon$ . We make the denoising model aware of the level of  
 123 noise through conditioning on a scalar  $\gamma$ . The proposed objective function for training  $f_\theta$  is

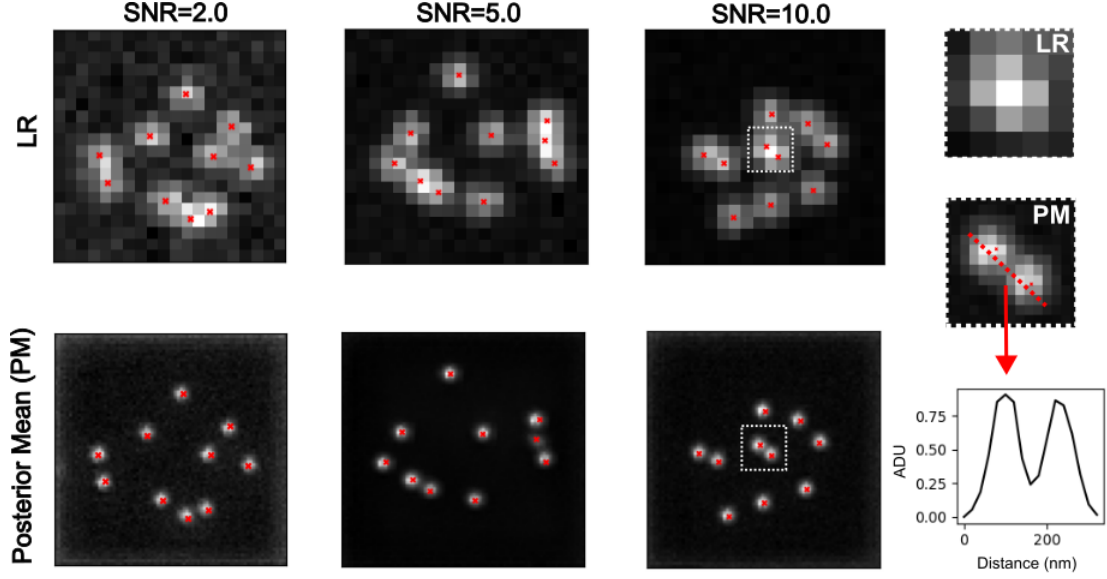


Figure 3: Kernel density estimates for various signal to noise ratios (SNR)

$$\mathbb{E}_{(\mathbf{z}, \mathbf{y}_0)} \mathbb{E}_{(\epsilon, \gamma)} \left[ f_{\theta} \left( x, \sqrt{\gamma} \mathbf{y}_0 + \sqrt{1 - \gamma} \epsilon \mid \mathbf{y}_t, \gamma \right) - \epsilon \right], \quad (14)$$

where  $\epsilon \sim \mathcal{N}(0, I)$ ,  $(\mathbf{z}, \mathbf{y}_0)$  is sampled from the training dataset and  $\gamma \sim p(\gamma)$ . The distribution of  $\gamma$  has a big impact on the quality of the model and the generated outputs. For our training noise schedule, we use a piecewise distribution for  $\gamma$ ,  $p(\gamma) = \frac{1}{T} \sum_{t=1}^T U(\gamma_{t-1}, \gamma_t)$  (Nanxin 2021). Specifically, during training, we first uniformly sample a time step  $t \sim \{0, \dots, T\}$  followed by sampling  $\gamma \sim U(\gamma_{t-1}, \gamma_t)$ . We set  $T = 100$  in all our experiments.

## 4 Experiments

We set  $T = 100$  for all experiments and treat forward process variances  $\beta_t$  as hyperparameters, with a linear schedule from  $\beta_0 = 10^{-4}$  to  $\beta_T = 10^{-2}$ . These constants were chosen to be small relative to data scaled to  $[-1, 1]$ , ensuring that reverse and forward processes have approximately the same functional form while keeping the signal-to-noise ratio at  $x_T$  as small as possible ( $L_T = D_{KL}(q(x_T|x_0) \parallel \mathcal{N}(0, I)) \approx 10^{-5}$  bits per dimension in our experiments).

To represent the reverse process, we used the DDPM architecture based on a U-Net backbone (Ho 2020). Parameters are shared across time, which is specified to the network using the Transformer sinusoidal position embedding ?. We use self-attention at the  $16 \times 16$  feature map resolution ?. Details are in Appendix A.

and the channel multipliers at different resolutions (see Appendix A for details). To condition the model on the input  $x$ , we up-sample the low-resolution image to the target resolution using bicubic interpolation. The result is concatenated with  $y_t$  along the channel dimension. We experimented with more sophisticated methods of conditioning, such as using, but we found that the simple concatenation yielded similar generation quality.

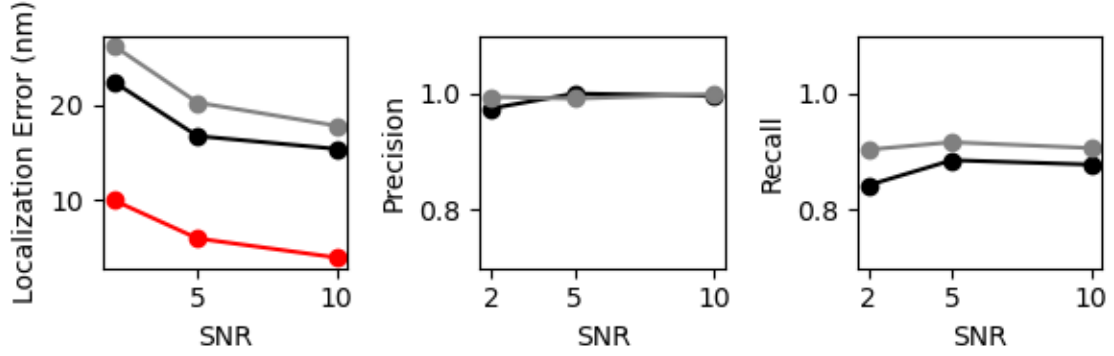


Figure 4: Localization precision and information retrieval

#### 144 4.1 Localization Error Analysis

### 145 5 Related Work

#### 146 5.1 Diffusion Models

147 Prior work of diffusion models ?? require 1-2k diffusion steps during inference, making generation  
 148 slow for large target resolution tasks. We adapt techniques from ? to enable more efficient inference.  
 149 Our model conditions on  $\gamma$  directly (vs  $t$  as in ?), which allows us flexibility in choosing the number  
 150 of diffusion steps, and the noise schedule during inference. This has been demonstrated to work  
 151 well for speech synthesis ?, but has not been explored for images. For efficient inference, we set the  
 152 maximum inference budget to 100 diffusion steps, and hyper-parameter search over the inference  
 153 noise schedule. This search is inexpensive as we only need to train the model once ?. We use FID on  
 154 held-out data to choose the best noise schedule, as we found PSNR did not correlate well with image  
 155 quality.

#### 156 5.2 Localization Microscopy with Deep Networks